

# Wide transparency range and high refractive index lead–niobium–germanate glass thin films

O. SANZ<sup>1</sup>  
J. GONZALO<sup>1,✉</sup>  
A. PEREA<sup>1</sup>  
J.M. FERNÁNDEZ-NAVARRO<sup>1</sup>  
C.N. AFONSO<sup>1</sup>  
J. GARCÍA LÓPEZ<sup>2</sup>

<sup>1</sup> Instituto de Óptica, CSIC, Serrano 121, 28006 Madrid, Spain

<sup>2</sup> Centro Nacional de Aceleradores, P. Tecnológico 'Cartuja 93', 41092 Sevilla, Spain

Received: 9 March 2004 / Accepted: 26 March 2004  
Published online: 2 June 2004 • © Springer-Verlag 2004

**ABSTRACT** Lead–niobium–germanate glass thin films have been produced by pulsed laser deposition in a broad O<sub>2</sub> pressure range (10<sup>-6</sup>–10<sup>-1</sup> mbar). The cation composition in the films approaches that of the glass target for a pressure of 10<sup>-2</sup> mbar. The oxygen content is only close to or above that of the glass for a pressure close to 10<sup>-1</sup> mbar, for which a Pb enrichment is also observed. Films grown in vacuum are highly absorbing, whereas transparent films with an absorption edge shifted to the UV with respect to the bulk glass are produced for pressures higher than 10<sup>-2</sup> mbar. The evolution of the optical energy gap and the refractive index of the films with the oxygen pressure is correlated to the changes observed in the film composition and discussed in terms of the features of the deposition process, the role of oxygen in the formation of the glass network and the progressive increase of the oxidation state of the cations as the oxygen pressure is increased.

PACS 81.05.Kf; 78.20.Ci; 81.15.Fg

## 1 Introduction

The development of all-optical communication technologies has opened new challenges to the design and production of materials suitable for the fabrication of both passive and active integrated devices. These materials should be able to operate not only in the standard communication windows but also at wavelengths beyond the transparency limit of fused silica. The range of envisaged applications includes optical waveguides for ultra-low-loss communications in the range 2.5–3.0 μm and more efficient lasers, amplifiers or nonlinear devices such as all-optical switches, among others [1–5].

Heavy metal oxide (HMO) glasses, characterized by their content of high molecular weight metal oxides, mainly Bi or Pb, exhibit physical properties that make them attractive candidates for these applications: long-term chemical stability when compared to other types of glasses [6], a broad transparency range in the near–mid-infrared spectral region and a low phonon energy (~ 800 cm<sup>-1</sup>) when compared to other oxide glasses [1–3, 7]. In particular, the low phonon energy

is very attractive for hosting rare-earth ions since it is essential to achieve long luminescence lifetimes and high quantum efficiencies [4, 5]. Furthermore, HMO glasses have high linear ( $n > 2$ ) and nonlinear ( $n_2 > 10^2$  times that of silica) refractive indices [1–3, 7]. The  $n_2$  value, although moderate when compared with composite materials containing metal or semiconductor nanoparticles, could be high enough for the development of integrated nonlinear devices in the near–mid infrared, since it is combined with low optical absorption and high  $n$  values. The latter leads to strong confinement of the light propagating in waveguides made of these glasses and, thus, to lower the power required to switch on the nonlinear response.

Different preparation methods have been attempted to produce high-quality oxide glass thin films such as sol–gel [8, 9], plasma- or laser-enhanced CVD [10, 11] or sputtering [12]. However, the production of high-quality HMO glass thin films is still a challenge. Pulsed laser deposition (PLD) is very attractive, since it is an excellent technique to produce complex oxide thin films with superior quality than other methods: high- $T_c$  superconductors and magnetic and nonlinear optical materials, among others [13, 14]. Nevertheless, it has scarcely been applied to the synthesis of complex oxide glasses [15–18].

One of the critical aspects in preparing such glasses is the limited transparency of the produced films in the wavelength range of interest, related to oxygen deficiencies that modify the glass structure. The oxygen content can be controlled in PLD through the use of an oxidant background gas during film deposition. However, the presence of the gas not only increases the oxygen content through chemical reactions at the surface of the growing film [19] or during the expansion of the plasma [20], but also modifies the plasma-expansion dynamics [21, 22] and the spatial distribution of the ejected material [23], which can have a negative impact on the structural properties of the films.

The aim of this work is to produce good-quality transparent and high refractive index HMO glass thin films. We have selected the PbO–Nb<sub>2</sub>O<sub>5</sub>–GeO<sub>2</sub> glass system in which GeO<sub>2</sub> and PbO are good stabilizers of the vitreous matrix, whereas Nb<sub>2</sub>O<sub>5</sub> increases the chemical stability and durability of the glass and improves its optical performance, both  $n$  and  $n_2$ . We have analyzed the influence of a gas pressure applied during

film growth and its reactive character on the stoichiometry and optical properties of the produced films.

## 2 Experimental

Lead–niobium–germanate (PbO–Nb<sub>2</sub>O<sub>5</sub>–GeO<sub>2</sub>) glass thin films have been produced by pulsed laser deposition using a KrF excimer laser beam ( $\lambda = 248$  nm,  $\tau = 12$  ns FWHM). The laser beam was focused at an angle of 45° on the surface of a rotating glass target to lead to an average energy density of  $2.5 \pm 0.5$  J/cm<sup>2</sup>. The vacuum chamber was evacuated prior to deposition to a residual pressure of  $6 \times 10^{-6}$  mbar. Film deposition took place in a wide O<sub>2</sub> pressure range ( $10^{-6}$ – $10^{-1}$  mbar) or in a fixed Ar pressure of  $5 \times 10^{-2}$  mbar on silicon, polycrystalline sapphire and soda-lime glass in order to match the different characterization techniques used in the present work. In all cases, the substrates were held at room temperature and the film thickness was in the 0.3–1.0- $\mu$ m range.

The target had a nominal composition of 25 PbO–15 Nb<sub>2</sub>O<sub>5</sub>–60 GeO<sub>2</sub> mol% and was obtained using standard melting methods. Batches of 20 g were prepared by mixing high-purity reagents: PbO (99.9995%), Nb<sub>2</sub>O<sub>5</sub> (99.999%) and GeO<sub>2</sub> (99.999%). The mixture was melted in a platinum crucible and placed in a furnace at a temperature of 1100–1300 °C for 1 h and then poured onto a brass plate, followed by 1 h of annealing at 450 °C and then cooled to room temperature at 1.5 °C/min. The resulting material was a transparent yellowish glass.

Nuclear microanalysis was used to determine the thickness and the elemental composition of the films. Nuclear reaction analysis (NRA) was used to determine the oxygen content of the films grown on silicon through the nuclear reaction <sup>16</sup>O(d, p)<sup>17</sup>O\* at 0.895 MeV. The absolute oxygen content was determined within 5% using a Ta<sub>2</sub>O<sub>5</sub>/Ta reference and the results were corrected for the contribution of the native SiO<sub>2</sub> layer present on the substrates. Cation contents were measured by Rutherford backscattering spectrometry (RBS) using a <sup>4</sup>He<sup>++</sup> beam at 5.93 MeV. Such a high beam energy was chosen to improve the mass resolution of the experiment. Further details of the compositional analysis of the films can be found elsewhere [18].

The optical characterization of films deposited on sapphire and soda-lime substrates has been performed by UV–visible absorption, spectroscopic ellipsometry and dark-mode spectroscopy. UV–visible absorption spectra were measured at normal incidence in the 350–1700-nm wavelength range using 5-nm steps. The absorption baseline corresponding to the substrates was subtracted in each case. The optical energy gap ( $E_g$ ) has been determined from the linear extrapolation to zero ordinate ( $(\alpha\hbar\omega)^{1/2} = 0$ ) of the Tauc formula [24]:

$$(\alpha\hbar\omega)^{1/2} = B(\hbar\omega - E_g), \quad (1)$$

where  $B$  is a constant,  $\alpha$  is the optical absorption and  $\hbar\omega$  is the photon energy. The ellipsometric parameters of the films,  $\tan \psi$  and  $\cos \delta$ , were determined using a WVASE J.A. Woollam Co. Inc. spectroscopic rotating analyzer ellipsometer in the 400–1700-nm wavelength range using 10-nm steps at two

angles of incidence: 60° and 66°. The real ( $n$ ) and imaginary ( $k$ ) parts of the refractive index were calculated from the ellipsometric parameters using a method described elsewhere [18]. Finally, dark-mode spectroscopy has been performed using a He–Ne laser beam coupled to the films by a rutile prism. The refractive index and the thickness of the films have been determined from the effective indices of at least two guided modes.

## 3 Results

Figure 1 shows the dependence of the relative content of each element,  $[X] = N_X/N_{\text{CAT}}$ , on the O<sub>2</sub> pressure applied during growth, where  $X = \text{Ge, Nb, Pb}$  and  $\text{O}$ ,  $N_X =$  number of atoms of element  $X$  and  $N_{\text{CAT}} =$  number of cations (Ge, Nb and Pb). At O<sub>2</sub> pressures lower than  $10^{-2}$  mbar, [Pb] is similar to that of the target whereas [Ge] and [Nb] are respectively above and below their respective contents in the target. From the results presented in Fig. 1 it is clear that films with cation contents close to that of the target can be obtained in a limited pressure range ( $\approx 1$ – $5 \times 10^{-2}$  mbar) for the experimental conditions considered in the present work. Finally, [Ge] decreases while [Pb] increases to values below and above those of the target respectively at pressures close to  $10^{-1}$  mbar.

The oxygen relative content, [O], does not depend significantly on the gas pressure up to  $10^{-3}$  mbar. The films are clearly oxygen deficient, [O] being only 50% that of the target in this low-pressure range. For O<sub>2</sub> pressures above  $10^{-2}$  mbar, [O] shows a significant increase, becoming close to that of the target for gas pressures in the range  $0.5$ – $1 \times 10^{-1}$  mbar. For comparison, the relative oxygen content measured for a film grown at an Ar pressure of  $5 \times 10^{-2}$  mbar has also been included in Fig. 1. This film has an [O] that is approximately 25% lower than that of the films grown at the same pressure but in O<sub>2</sub>.

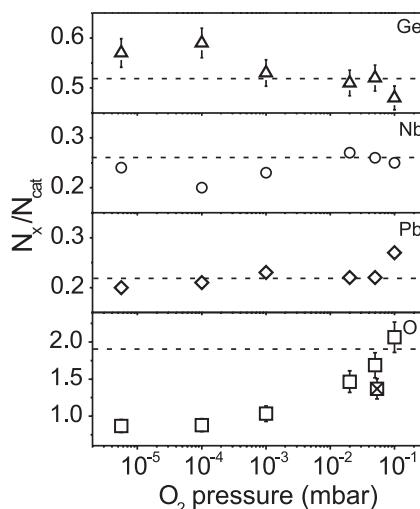


**FIGURE 1** Relative content of each element,  $X = \text{Ge, Nb, Pb}$  and  $\text{O}$ , as a function of the oxygen pressure applied during deposition, where  $N_X =$  number of atoms of element  $X$  and  $N_{\text{CAT}} =$  number of cations. The dashed line corresponds in each case to the respective relative content in the target. The crossed symbol ( $\boxtimes$ ) in the case of  $X = \text{O}$  corresponds to a sample grown in Ar

Figure 2 shows the UV–visible transmittance spectra for films grown at increasing O<sub>2</sub> pressures in the range 10<sup>−4</sup> to 10<sup>−1</sup> mbar. The oscillations observed in the spectra are produced by interference phenomena between the light reflected at the air–film and film–substrate interfaces. Transmittance of films grown at lower O<sub>2</sub> pressures, not shown in Fig. 2, shows features similar than those of films grown at 10<sup>−4</sup> mbar: low transmittance (< 0.5) and an absorption edge well in the visible. The film transmittance increases as the O<sub>2</sub> pressure increases, reaching a maximum for films grown at ≈ 5 × 10<sup>−2</sup> mbar of O<sub>2</sub>. The absorption edge presents a more complex dependence on the O<sub>2</sub> pressure. It shifts to higher photon energies as the O<sub>2</sub> pressure increases, reaching a maximum value for 5 × 10<sup>−2</sup> mbar. For pressures above this value, the absorption edge shifts back towards smaller photon energies, as is illustrated in Fig. 2 for the film grown at 10<sup>−1</sup> mbar. This is more clearly seen in Fig. 3, where the optical energy gap (E<sub>g</sub>) has been plotted as a function of the oxygen pressure. To illustrate the procedure followed in the determination of E<sub>g</sub>, the inset in Fig. 3 shows the Tauc plots for the bulk target (B) and for a film grown at 5 × 10<sup>−2</sup> mbar of O<sub>2</sub> (F). Figure 3 shows that E<sub>g</sub> remains constant and close to 1 eV, and thus well below the value for the bulk glass (≈ 2.97 eV), for O<sub>2</sub> pressures below 10<sup>−3</sup> mbar. Above 10<sup>−3</sup> mbar, E<sub>g</sub> increases as the O<sub>2</sub> pressure increases to reach a maximum value (E<sub>g</sub> = 3.64 eV) for an O<sub>2</sub> pressure of 5 × 10<sup>−2</sup> mbar. A further increase of the oxygen pressure reduces the value of E<sub>g</sub>, to approach that of the bulk glass for 10<sup>−1</sup> mbar. The E<sub>g</sub> measured for the film grown at 5 × 10<sup>−2</sup> mbar of Ar is included in Fig. 3 for comparison, the value being significantly lower than the

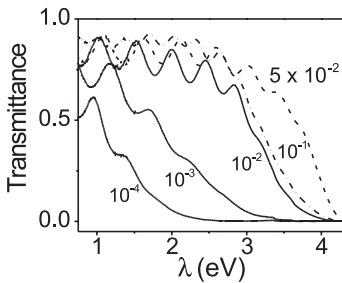


FIGURE 2 Transmittance spectra of films grown at increasing O<sub>2</sub> pressures (in mbar)

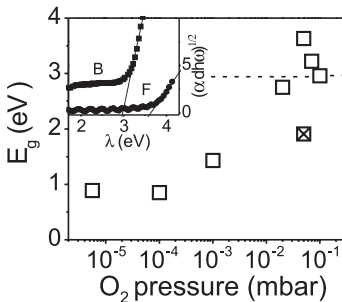


FIGURE 3 Optical energy gap (E<sub>g</sub>) as a function of the O<sub>2</sub> pressure applied during deposition. The dashed line corresponds to the E<sub>g</sub> value of the bulk glass whereas the crossed symbol (⊠) corresponds to the E<sub>g</sub> value of a sample grown in Ar. The inset shows the Tauc plots for the bulk glass (B) and for a film (F) grown at 5 × 10<sup>−2</sup> mbar of O<sub>2</sub>. Tauc plots have been multiplied in both cases by d<sup>1/2</sup>, where d is the sample thickness, in order to bring the data for B and F into the same scale

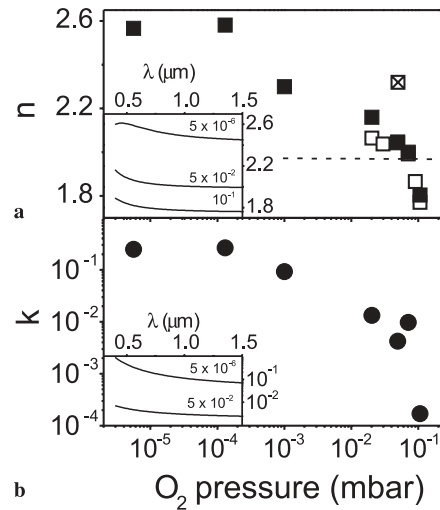


FIGURE 4 a Real, *n*, and b imaginary, *k*, parts of the refractive index as a function of the oxygen pressure applied during deposition, determined from ■, ●, ⊠ ellipsometric measurements at λ = 630 nm and □ dark-mode spectroscopy at λ = 633 nm. The *n* value measured for a sample grown in Ar (⊠) and the *n* value of the bulk glass (dashed line) are included in (a). The insets show the spectral dependence of a *n* and b *k* for films grown at representative O<sub>2</sub> pressures (in mbar). The *k* value for the film grown at 10<sup>−1</sup> mbar (≤ 10<sup>−4</sup>) has been represented in (b) by the value of the resolution threshold of the experimental set-up (≈ 10<sup>−4</sup>)

one corresponding to films grown at 5 × 10<sup>−2</sup> mbar of O<sub>2</sub>. In fact, the value of E<sub>g</sub> in Ar is close to that of films grown at reduced (10<sup>−3</sup> mbar) O<sub>2</sub> pressures.

The dependence of the real (*n*) and imaginary (*k*) parts of the refractive index of the films at 630 nm on the O<sub>2</sub> pressure applied during growth is shown in Fig. 4. The insets show the spectral dependence of *n* and *k* for representative films. In all cases, *n* shows a smooth spectral dependence, which follows a negative dispersion law. The overall value of *n* decreases when increasing the O<sub>2</sub> pressure as shown in Fig. 4a. Values of *n* obtained at 633 nm using dark-mode spectroscopy have also been included in Fig. 4a, the agreement with the values obtained from ellipsometry being very good. Films grown at low O<sub>2</sub> pressures (≤ 10<sup>−4</sup> mbar) have a value of *n* close to 2.6, whereas *n* decreases steadily for O<sub>2</sub> pressures above 10<sup>−2</sup> mbar to reach a value of *n* = 1.8 at 10<sup>−1</sup> mbar. The value of *n* for films grown at 5 × 10<sup>−2</sup> mbar is similar to that of the bulk glass (1.98). The imaginary part of the refractive index (Fig. 4b) shows a similar qualitative dependence on the O<sub>2</sub> pressure to *n*, since it decreases when the O<sub>2</sub> pressure increases. Films grown at low O<sub>2</sub> pressures are highly absorbent in the whole studied spectral range (*k* ≥ 10<sup>−1</sup>), as shown in the inset of Fig. 4b. Films grown at 5 × 10<sup>−2</sup> mbar have a value of *k* close to 5 × 10<sup>−3</sup> in all the spectral range while the value of *k* falls below the resolution threshold of our measurements (*k* ≈ 10<sup>−3</sup>) for films grown at 10<sup>−1</sup> mbar.

#### 4 Discussion

The results presented in this work clearly show that the presence of an oxygen background has a strong influence on the quality of lead–niobium–germanate glass films produced by PLD, since both the composition and the optical properties strongly depend on the gas pressure applied dur-

ing growth. Even for a pressure of  $10^{-2}$  mbar, for which the cation proportion is similar to that of the bulk glass, the oxygen content is lower than the one expected. This is a critical issue since oxygen is a key element for the formation of the glass network as it may enter in the network either as bridging or non-bridging ions [25].

Films deposited in vacuum are opaque brown, whereas they become transparent at a pressure close to  $10^{-2}$  mbar and yellowish for  $10^{-1}$  mbar, similarly to what has earlier been reported for other lead-germanate films produced by PLD [17]. The brown color obtained when growing in vacuum was tentatively related in that work to oxygen deficiencies, although no experimental evidence was provided. The results shown in Fig. 1 confirm such a hypothesis since films grown in vacuum present a severe [O] deficiency close to 50%. Therefore, they contain less than one oxygen atom per cation and, thus, a low oxidation state of Pb, Ge and Nb ions in the films can be expected. Furthermore, some metal segregation cannot be ruled out. Under these conditions, the formation of the glass network is most likely prevented. Instead, a mixture of amorphous low-valence and sub-stoichiometric oxides, that fits better the compositional results shown in Fig. 1, might be the main constituent of the films. This interpretation is consistent with the high absorption shown in Fig. 4b and the reduced transparency-interval and energy-gap values shown in Figs. 2 and 3 for films grown in vacuum or low  $O_2$  pressures.

The presence of an oxidant environment at pressures  $\geq 10^{-2}$  mbar induces a significant increase of [O] as shown in Fig. 1. The fact that films grown at  $5 \times 10^{-2}$  mbar of  $O_2$  exhibit [O] values higher than the film grown at the same Ar pressure clearly indicates that a significant incorporation of oxygen to the films is taking place from the  $O_2$  environment. Processes that may take place during the film growth at the substrate or the expansion of the plasma mainly determine this incorporation. On the one hand, the existence of surface oxidation reactions at the substrate has been reported in the PLD growth of amorphous  $GeO_2$  films [19]. On the other hand, the formation of oxides during the expansion of the plasma in an  $O_2$  environment [20] helps to increase the oxygen content of the films in the case of high- $T_c$  superconductors and other oxides. The probability of such formation to occur relates to the reaction exothermicities of the possible monoxides that in this work have been calculated according to the model developed by Gupta [26], and summarized in Table 1 for the present case. It is seen that the formation of NbO and GeO by chemical reaction of the corresponding cations with  $O_2$  is exothermic and, thus, very likely to occur. Instead, the formation of PbO is an endothermic process, which however could be possible due to the fact that a fraction of the Pb atoms (or

ions) present in the plasma have a kinetic energy high enough to activate such a chemical reaction [20]. Moreover, the possible dissociation of  $O_2$  molecules by electronic impact very close to the target at the early stages of the plasma expansion [27] could provide an additional source to enhance the oxidation processes.

In this pressure range ( $10^{-2}$ – $10^{-1}$  mbar), the expansion of the transient plasma is dominated by the scattering of the ejected species by the background-gas molecules [21, 22] and, thus, this process determines their trajectory and kinetic energy. The formation of monoxides in the gas phase will contribute then to the increase of the overall [O] in the films, since monoxides should suffer lower angular scattering than atomic oxygen, due to their higher mass with respect to atomic oxygen. Moreover, this process will preferentially broaden the distribution of the lightest cation (Ge) with respect to the heaviest one (Pb) and, as a consequence, an increase of the heavy-to-light cation concentration ratio is expected at the center of the deposit. This increase is more important the higher the pressure, in good agreement with the evolution of cation contents shown in Fig. 1.

The optical response of the films improves when increasing the  $O_2$  pressure up to  $10^{-2}$  mbar, this improvement being consistent with the increase of [O]. At  $10^{-2}$  mbar, both  $E_g$  and  $n$  become similar to those of the bulk glass, thus suggesting that [O] is high enough to enable the formation of the glass structure. A further pressure increase up to  $5 \times 10^{-2}$  mbar leads to a maximum value of  $E_g$  that is well above the value for the bulk glass. This behavior is undoubtedly related to the structural and compositional changes induced by the increase of [O] in the films, although [O] is still lower than that of the target as shown in Fig. 1. Therefore, this result suggests that the glass structure should be different to that of the bulk glass, i.e. the constituent oxides must have a lower oxidation state than that of the oxides in the bulk glass, but higher than that of the oxides forming the films deposited in vacuum. Since glasses with such oxide mixtures are not formed under standard bulk glass preparation techniques, this result is most likely related to the capability of PLD to produce metastable mixture phases [18]. The presence of PbO and  $GeO_2$  together with  $NbO_2$  (instead of  $Nb_2O_5$ ) in the films produced at  $5 \times 10^{-2}$  mbar would decrease the required [O] content to make it consistent with the experimentally determined values. The optical behavior of films deposited at  $5 \times 10^{-2}$  mbar of Ar agrees well with the above interpretation, since their measured  $E_g$  (Fig. 3) and  $n$  (Fig. 4a) values are similar to those of films grown at lower  $O_2$  pressures, which indeed have a reduced [O] as shown in Fig. 1.

At  $10^{-1}$  mbar, the observed increase of [Pb] together with the fact that [O] is above the corresponding value for the bulk glass suggest that Pb might be further oxidized to less polarizable  $Pb^{4+}$  ions, this leading to the formation of  $PbO_2$  in the films as neither Ge nor Nb can have a higher oxidation state than the one they have in the bulk target. The substitution of PbO by  $PbO_2$  in bulk glasses has proven to have a significant effect on their optical properties, as a decrease of  $E_g$  and  $n$  can be expected [28]. Therefore, the observed decrease of  $E_g$  and, consequently, the red shift of the absorption edge are most likely related to the formation of  $PbO_2$  in the films produced at  $10^{-1}$  mbar.

	$E$ (eV)	$\sigma$ ( $\times 10^{-16}$ cm <sup>2</sup> )
NbO	2.82	49
GeO	1.66	43
PbO	-1.22	53

**TABLE 1** Reaction exothermicities ( $E$ ) and total scattering cross sections ( $\sigma$ ) for the formation of Ge, Nb and Pb monoxides in reaction with  $O_2$ . The values are estimated according to the model proposed in [26]. The negative sign indicates that the reaction is endothermic

Finally, the observed decrease of both the real ( $n$ ) and the imaginary ( $k$ ) parts of the refractive index with the O<sub>2</sub> pressure applied during growth, which becomes sharper above 10<sup>-2</sup> mbar (see Fig. 4), is not only related to the incorporation of oxygen to the films, but also to the influence that the presence of a background gas has on the deposition process. First, the increase of [O] in the films decreases their absorption, as it allows the formation of the glass structure, whereas it induces a decrease of the value of  $n$  at pressures above 5 × 10<sup>-2</sup> mbar due to the further oxidation of lead [28]. Secondly, there is a process intrinsic to PLD that is known to influence the refractive index: in vacuum, the high kinetic energy of the species arriving to the substrate is known to produce optically dense films and, thus, films with an enhanced value of  $n$ . The presence of a background gas reduces this kinetic energy, leading to a decrease of the value of  $n$  for films as observed in Fig. 4 when increasing the O<sub>2</sub> pressure during growth.

## 5 Conclusions

Lead–niobium-germanate thin films have been produced by PLD in a broad O<sub>2</sub> pressure range (10<sup>-6</sup>–10<sup>-1</sup> mbar). The production of glass films formed by oxide mixtures different from those of the target is most likely related to the ability of PLD to produce mixture or metastable phases that are not achievable by bulk production methods. Transparent films with an absorption edge shifted to the UV with respect to that of the bulk glass and similar refractive index are achieved when using an O<sub>2</sub> background in the 5 × 10<sup>-2</sup>–10<sup>-1</sup> mbar pressure range. The evolution of the optical properties with the O<sub>2</sub> pressure is related to the progressive increase of the [O] content in the films that induces an increase of the oxidation state of the cations. The decrease of  $E_g$  and the red shift of the absorption edge observed for films grown at 10<sup>-1</sup> mbar are related to the observed increase of [Pb] in the films, this increase being most likely accompanied by a further oxidation of Pb<sup>2+</sup> ions (PbO) to less polarizable Pb<sup>4+</sup> ones (PbO<sub>2</sub>).

Finally, the sharp decrease of the real part of the refractive index of films for O<sub>2</sub> pressures above 10<sup>-2</sup> mbar is related to the combined effect of the formation of PbO<sub>2</sub> in the glass films and the decrease of the kinetic energy of the species arriving to the substrate, which is characteristic of PLD in that gas-pressure regime.

**ACKNOWLEDGEMENTS** This work has been partially funded by the Spanish Ministry of Science and Technology (Project No. MAT2000-1135-C02-02). O. Sanz acknowledges a grant from the Comunidad Autónoma de Madrid, Spain.

## REFERENCES

- 1 W.H. Dumbaugh, J.C. Lapp: *J. Am. Ceram. Soc.* **75**, 2315 (1992)
- 2 M.E. Lines: *J. Appl. Phys.* **69**, 6876 (1991)
- 3 E.M. Vogel, M.J. Weber, D.M. Krol: *Phys. Chem. Glasses* **32**, 231 (1991)
- 4 D.R. MacFarlane, P.J. Newman, R. Plathe, D.J. Booth: *SPIE* **3849**, 94 (1999)
- 5 H. Takebe, K. Yoshino, T. Murata, K. Morinaga, J. Hector, W.S. Brocklesby, D.W. Hewak, J. Wang, D.N. Payne: *Appl. Opt.* **36**, 5839 (1997)
- 6 M.J. Liepmann, N. Neuroth: 'Infrared-transmitting Glasses'. In: *The Properties of Optical Glass*, ed. by M. Bach, N. Neuroth (Springer, Berlin 1995)
- 7 S. Sakka: *Glass Phys. Chem.* **24**, 257 (1998)
- 8 E.R. La Serra, Y. Charbouillot, P. Baudry, M.A. Aegerter: *J. Non-Cryst. Solids* **121**, 323 (1990)
- 9 G.C. Righini, A. Verciani, S. Pelli, M. Guglielmi, A. Martucci, J. Fick, G. Vitrant: *Pure Appl. Opt.* **5**, 655 (1996)
- 10 F. Ay, A. Aydinli, S. Agan: *Appl. Phys. Lett.* **83**, 4743 (2003)
- 11 M. Kubo, H. Hanabusa: *Appl. Opt.* **29**, 2755 (1990)
- 12 P. Mazzoldi, G.C. Righini: in *Insulating Materials for Optoelectronics: New Developments*, ed. by F. Agulló-López (World Scientific, Singapore 1995) Chap. 13 and references therein
- 13 K.L. Saenger: in *Pulsed Laser Deposition*, ed. by D.B. Chrisey, G.K. Hubler (Wiley, New York 1994) p. 582
- 14 C.N. Afonso: in *Insulating Materials for Optoelectronics: New Developments*, ed. by F. Agulló-López (World Scientific, Singapore 1995) Chap. 1 and references therein
- 15 E.M. Vogel, E.W. Chase, J.L. Jackel, B.J. Wilkens: *Appl. Opt.* **28**, 649 (1989)
- 16 C.N. Afonso, J.M. Ballesteros, J. Gonzalo, G.C. Righini, S. Pelli: *Appl. Surf. Sci.* **96–98**, 760 (1996)
- 17 S. Mailis, Ch. Riziotis, J. Wang, E. Taylor, A.A. Anderson, S.J. Barrington, H.N. Rutt, R.W. Eason, N.A. Vainos, Ch. Grivas: *Opt. Mater.* **12**, 27 (1999)
- 18 J. Gonzalo, O. Sanz, A. Perea, J.M. Fernandez-Navarro, C.N. Afonso, J. García López: *Appl. Phys. A* **76**, 743 (2003)
- 19 S. Witanachchi, P.J. Wolf: *J. Appl. Phys.* **76**, 2185 (1994)
- 20 C.E. Otis, A. Gupta, B. Braren: *Appl. Phys. Lett.* **62**, 102 (1993)
- 21 D.B. Geohegan: in *Pulsed Laser Deposition*, ed. by D.B. Chrisey, G.K. Hubler (Wiley, New York 1994) Chap. 5 and references therein
- 22 J. Gonzalo, C.N. Afonso, J.M. Ballesteros, A. Grossman, C. Ortega: *J. Appl. Phys.* **82**, 3129 (1997)
- 23 K.L. Saenger: in *Pulsed Laser Deposition*, ed. by D.B. Chrisey, G.K. Hubler (Wiley, New York 1994) Chap. 7 and references therein
- 24 X. Liu, D.B. Hollis, J. McDougall: *Phys. Chem. Glasses* **37**, 160 (1996)
- 25 N. Neuroth: in *The Properties of Optical Glass*, ed. by H. Bach, N. Neuroth (Springer, Berlin 1995) p. 59
- 26 A. Gupta: *J. Appl. Phys.* **73**, 7877 (1993)
- 27 A. Camposeo, F. Cervelli, F. Fusco, M. Allegrini, E. Arimondo: *Appl. Phys. Lett.* **78**, 2402 (2001)
- 28 W. Vogel: *Glaschemie* (Springer, Berlin 1992)